Title
Bistable dynamics of turbulence spreading in a corrugated temperature profile

Journal
Physics of Plasmas, 24(10)

ISSN
1070-664X

Authors
Guo, ZB
Diamond, PH

Publication Date
2017-10-01

DOI
10.1063/1.5000850

Bistable dynamics of turbulence spreading in a corrugated temperature profile

Z. B. Guo, and P. H. Diamond

Citation: Physics of Plasmas **24**, 100705 (2017); doi: 10.1063/1.5000850
View online: http://dx.doi.org/10.1063/1.5000850
View Table of Contents: http://aip.scitation.org/toc/php/24/10
Published by the American Institute of Physics

Bistable dynamics of turbulence spreading in a corrugated temperature profile

Z. B. Guo[a] and P. H. Diamond
University of California, San Diego, California 92093, USA

(Received 18 August 2017; accepted 26 September 2017; published online 5 October 2017)

We present a new model of turbulence spreading in magnetically confined plasma. A basic question in turbulence spreading is how to sustain finite amplitude fluctuations in a stable subcritical region, where linear dissipation of the turbulence is strong? The answer to this question relies on a consistent treatment of mesoscale temperature profile corrugation and microscale turbulence. We argue that inhomogeneous mixing of the turbulence corrugates the mean temperature profile and that the temperature corrugation then induces subcritical bifurcation of the turbulence. Thus, the system will transition from a metastable "laminar" state to an absolutely stable, excited state. Incorporating spatial coupling of the locally excited turbulent regions, a front forms. This front connects the excited and laminar states and penetrates the linear stable region efficiently. We argue that such bistable turbulence spreading can explain observations of hysteresis in the intensity of L-mode core turbulence. *Published by AIP Publishing.* https://doi.org/10.1063/1.5000850

A longstanding issue in anomalous transport in magnetically confined plasma systems is how turbulent fluctuations may penetrate stable regions (e.g., a transport barrier), where the free energy is incapable of driving linear instabilities. The mechanism most frequently involved for this is so-called turbulence spreading.[1–5] Turbulence spreading provides a natural way to contaminate stable domains,[6] as in the H → L transition phenomena.[7] Most previous works treat turbulence spreading as a Fisher front. But Fisher fronts are in fact heavily damped in the subcritical domains (shown below) and so do not effectively penetrate these. Thus, an improved treatment of the turbulence spreading is necessary. To achieve a sufficient penetration depth, a way to subcritically excite local turbulence is needed. In this work, we show that inhomogeneous mixing—specifically mesoscale corrugation of the temperature profile—can provide such nonlinear drive. Hence, this new model of *bistable* turbulence spreading is constructed.

First, we briefly discuss the "standard model"—based on nonlinear Fisher fronts—of turbulence spreading. This has the generic structure[8]

$$\frac{\partial}{\partial t}I = \gamma_l I - \gamma_{nl} I^2 + \frac{\partial}{\partial x} D_{nl} \frac{\partial}{\partial x} I, \tag{1}$$

where $\gamma_l I$ is a linear driving term. Here, the linear growth rate γ_l is proportional to the mean temperature gradient. $\gamma_{nl} I^2$ is a local nonlinear saturation term. $D_{nl} \propto I$ is the nonlinear diffusion term, which describes spatial coupling of the turbulence field. In the linearly unstable regime, there are two homogeneous, steady solutions for Eq. (1): $I = 0$ (unstable) and $I = \gamma_l/\gamma_{nl}$ (stable). Otherwise, I either decays as $I \propto t^{-1}$ in the near marginal region ($\gamma_l \sim 0$) or exponentially $I \propto e^{\gamma_l t}$ in the subcritical region ($\gamma_l < 0 \,\&\, |\gamma_l| > \gamma_{nl} I$). Therefore, the Fisher turbulence spreading front suffers strong damping in the subcritical region, so the depth that the turbulence can penetrate into this region is quite limited. The resolution of this dilemma of Eq. (1) relies on incorporating the nonlinear drive effect of the turbulence field, i.e., including a treatment of how the spreading front modifies the local gradient and stability as it passes. This induces *bistability* of the turbulence, in contrast to the Fisher model, which is *unistable*. In this work, we show that temperature profile corrugation can provide such a nonlinear drive and so sustain a finite amplitude of turbulence intensity in the subcritical region. This enables turbulence spreading and reconciles $\gamma_l < 0$ with that phenomenon.

Temperature corrugations in magnetically confined plasma systems have long been observed.[9] These were generally believed to play a secondary role in the supercritical region and usually were dismissed in various anomalous transport models. An exception is Ref. 10. In this work, we show that the temperature corrugation plays an essential role in driving turbulence penetration of the subcritical region, i.e., it can overcome the local damping and hence allow efficient turbulence spreading. The underlying physics mechanism is (Fig. 1) *inhomogeneous turbulent mixing*,[11] which reduces the turbulent heat flux at certain locations while increasing the temperature gradient at adjacent locations. This is equivalent to inducing a negative heat flux on mesoscales. Thermal energy then accumulates near such locations, so that the temperature gradient sharpens locally, resulting in the formation of corrugations. These temperature corrugations will enhance the local temperature gradient drive and so induce local turbulence excitation. A significant difference from the traditional Fisher model is that both the excited state and the "laminar" state are stable, i.e., the system is *bistable*. Thus, a stable turbulence front forms and spreads. Bistability of the turbulence—the core of our model—has been observed in experiment.[12] Inagaki *et al.* discovered an *S*-curve relation between the turbulence

[a]Author to whom correspondence should be addressed: guozhipku@gmail.com

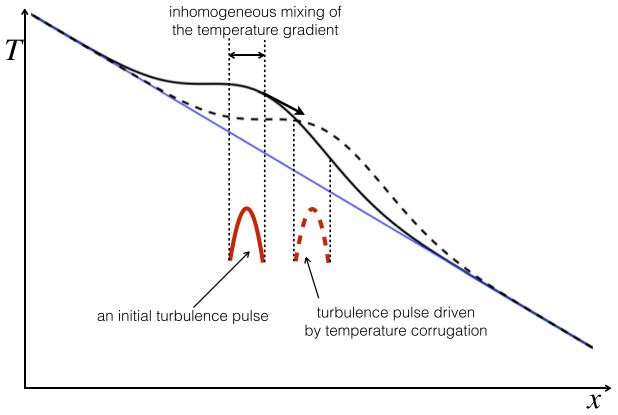

FIG. 1. Sketch of bistable turbulence spreading induced by inhomogeneous mixing. Blue line: subcritical mean temperature profile.

intensity and the temperature gradient, which strongly suggests turbulence bistability. Note that while bistable *S*-curve relations, linking flux and gradient, have long been observed, this corresponding observation for *fluctuation intensity in the L-mode (without internal transport barrier observed!) is unique*.

Incorporating the nonlinear drive of temperature corrugations, Eq. (1) is revised to the following form ($A \equiv -\partial_x T$):

$$\frac{\partial}{\partial t} I = \gamma_0 \left(\langle A \rangle + \Theta(\tilde{A}_m)\tilde{A}_m - A_C \right) I - \gamma_{nl} I^2 + D_1 \frac{\partial}{\partial x}\left(I \frac{\partial}{\partial x} I \right), \tag{2}$$

where the linear growth rate is explicitly written as $\gamma_l = \gamma_0(\langle A \rangle - A_C)$ with $\langle A \rangle$ being the mean temperature gradient and A_C the critical gradient. Note: more precisely, $L_T^{-1}(L_T^{-1} \equiv -\partial_x lnT)$ is the drive term, and it has a similar trend to A. The incremental temperature gradient induced by the profile corrugation is denoted as $\tilde{A}_m$. Since only a positive temperature gradient corrugation acts as a drive, a step function $\Theta(\tilde{A}_m)$ is introduced in Eq. (2). A negative corrugation would render the turbulence stable. Note that the local nonlinear saturation is composed of two processes: ZF flow shear ($\propto |\langle V_{ZF} \rangle'| I$) and mode-mode coupling ($\propto I^2$). Since the amplitude of zonal flow shear is proportional to the turbulence intensity gradient via Reynolds stress, i.e., $|\langle V_{ZF} \rangle'| \propto I' = L_I^{-1} I (L_I \equiv I'/I$–the characteristic scale of the turbulence intensity envelope), the local saturation term is written as $\gamma_{nl} I^2$. Now γ_{nl} is a coefficient which includes both mode-mode coupling and zonal flow shearing effects. Equivalently, the zonal flow shear effect can also be related to a nonlinear shift of the threshold A_C, i.e., $A_C \to A_C + \Delta A_C$ and $\Delta A_C \propto |\langle V_{ZF} \rangle'| \propto I$. The nonlinear diffusivity is written as $D_{nl} = D_1 I$ with D_1 being a coefficient. *Note*: $\langle \ldots \rangle$ should be understood as a double average, i.e., $\langle \ldots \rangle \equiv \langle \langle \ldots \rangle_s \rangle_m$ with $\langle \ldots \rangle_s$ being an average over micro-timescales and $\langle \ldots \rangle_m$ over mesoscales (i.e., the corrugation scale). A simple observation of Eq. (2) is that, in the subcritical region ($\langle A \rangle < A_C$), a strong enough temperature corrugation can induce the local excitation of the turbulence. To know "how strong is strong?," one needs a relation between the corrugation strength and the turbulence intensity, which constitutes a "closure" of Eq. (2).

To obtain the relation between $\Theta(\tilde{A}_m)\tilde{A}_m$ and I, we start from the temperature evolution equation

$$\frac{\partial}{\partial t} T + \nabla \cdot Q_T = \frac{\partial}{\partial x}\left(\chi_{neo} \frac{\partial}{\partial x} T \right) + S_{inj}\delta(x), \tag{3}$$

where $Q_T = \tilde{\mathbf{v}} T$ is the turbulent heat flux with being $\tilde{\mathbf{v}}$ the $E \times B$ convection velocity. S_{inj} accounts for the heating (centroid, $x = 0$). For the background heat flux in Eq. (3), the neoclassical term ($\chi_{neo}\partial_x T$) is retained.[13] As compared with the conventional form of the temperature evolution equation,[13] a factor 2/3 was absorbed into χ_{neo} and inter-species thermal coupling was ignored. Multiplying by T on both sides of Eq. (3) and carrying out the double average, one obtains the corrugation strength

$$\langle \tilde{A}_m^2 \rangle \chi_{neo} \simeq \langle A \rangle \langle Q_T \rangle + \langle \tilde{A}_m \tilde{v}_x \tilde{T} \rangle. \tag{4}$$

In this work, we are interested in how strongly the turbulence intensity is excited and how far it spreads, for a given corrugated profile. As we explore the effect of a statistical ensemble of temperature corrugations, approximation $\partial_t \langle \tilde{A}^2 \rangle \simeq 0$ was used in deriving Eq. (4). In obtaining Eq. (4), we assumed $\langle \tilde{T}_m^2 \rangle \gg \langle \tilde{T}_s^2 \rangle$ with $\tilde{T}_s$ temperature fluctuation at the microscale. The triple coupling term in Eq. (4) reflects meso- and micro-scale coupling and so contains the physics of temperature corrugation. With the double average, it follows that $\langle \tilde{A}_m \tilde{v}_x \tilde{T} \rangle = \langle \tilde{A}_m \langle \tilde{v}_x \tilde{T} \rangle_s \rangle_m = \langle \tilde{A}_m \tilde{Q}_{T,m} \rangle_m$, and $\tilde{Q}_{T,m}$ is the mesoscale turbulent heat flux. A natural way to induce mesoscale temperature corrugation is inhomogeneous turbulent mixing. This also is the most general way to understand zonal flow structure generation.[14] We remark here that there are other ways to generate temperature gradient corrugations, such as by the finite time delay effect between $\tilde{Q}_m$ and $\partial_x \tilde{T}_m$,[15] by magnetic islands,[16] and so on. Via inhomogeneous mixing, the turbulent heat flux in the strong zonal flow shear region drops, so the thermal energy "piles up" around the shear layer and temperature profile steepens locally and so is corrugated. An important detail is that zonal shear $\propto \partial_x^2 \tilde{T}_m$(from local radial force balance), relevant when the dominant nonlinear process is the zonal flow–turbulence interaction (Fig. 1). The temperature corrugation $\propto \partial_x \tilde{T}_m$, where the ∇T and I interaction is dominant. Therefore, zonal shear and mesoscale temperature gradient drive act at somewhere different, but nearby, locations. As we focus how the temperature corrugations impact turbulence excitation, the zonal shear evolution is not included explicitly. The process of corrugation formation is equivalent to a secondary flux that is locally "up" the mesoscale temperature gradient, i.e., $\tilde{Q}_{T,m}\partial_x \tilde{T}_m > 0$. With the Fickian approximation, $\tilde{Q}_{T,m}$ can be written as $\tilde{Q}_{T,m} = -\chi_m \partial_x \tilde{T}_m$. χ_m is a "negative" thermal conductivity,[17] which reflects the up-gradient feature of the mesoscale heat flux. Such negative conductivity is rooted in the bistability of the system. The triple coupling term in Eq. (4) then follows as $\langle \tilde{A}_m \tilde{v}_x \tilde{T} \rangle = -|\chi_m| \langle \tilde{A}_m^2 \rangle$. χ_m is determined by the detailed process of the inhomogeneous turbulent mixing process, i.e., pumping of the mesoscale temperature field by turbulence. In fact, due to the natural connection between $\partial_x^2 \tilde{T}_m$ and zonal shear, we can expect that χ_m would resemble

the "negative" viscosity, which characterizes secondary growth as in the modulational instability of a seed zonal shear. The mean turbulent heat flux is $\langle Q_T\rangle = -\chi_T\partial_x\langle T\rangle = \chi_T\langle A\rangle$, where the turbulent thermal conductivity has a form $\chi_T = D_0 I$ with D_0 being a coefficient. Since the underlying physics of both the heat conductivity (D_0) and the turbulent scattering diffusivity (D_1) is the same (i.e., mode coupling induced turbulent mixing), we have $D_0 \simeq D_1$. Substituting $D_0 I\langle A\rangle$ for $\langle Q_T\rangle$ and $-|\chi_m|\langle\tilde{A}_m^2\rangle$ for $\langle\tilde{A}_m\tilde{v}_x\tilde{T}\rangle$ in Eq. (4) yields

$$\langle\tilde{A}_m^2\rangle = \frac{D_0\langle A\rangle^2}{\chi_{neo}+|\chi_m|}I. \tag{5}$$

Equation (5) is a generalized Zeldovich relation,[18] and it indicates that the temperature corrugation strength is proportional to the turbulence intensity. With Eq. (2), the "loop" of the model is now closed.

To have a more physical understanding of how temperature corrugation impacts turbulence excitation and spreading into the subcritical region, we keep only the averaged drive effect in Eq. (2), i.e., $\Theta(\tilde{A}_m)\tilde{A}_m \simeq \langle\Theta(\tilde{A}_m)\tilde{A}_m\rangle$. This is valid when the variation of the corrugations at different locations is relatively small. Then, one has $\langle\Theta(\tilde{A}_m)\tilde{A}_m\rangle \simeq \sqrt{\langle\tilde{A}_m^2\rangle}$. Substituting it into Eq. (2) and employing Eq. (5) yield

$$\frac{\partial}{\partial t}I = \gamma_0(\langle A\rangle - A_C)I + \sqrt{\frac{\gamma_0^2 D_0\langle A\rangle^2}{\chi_{neo}+|\chi_m|}}I^{3/2} - \gamma_{nl}I^2 + D_1\frac{\partial}{\partial x}\left(I\frac{\partial}{\partial x}I\right). \tag{6}$$

Without the temperature corrugation effect (2nd term on the RHS), Eq. (6) has the conventional Fisher form, i.e., reduces to Eq. (1). But Eq. (6) now contains a new term, which results from the treatment of corrugation. Equation (6) is driven by two processes: local turbulence excitation and turbulence spreading. The spatial coupling term in Eq. (6) has two consequences: steepening [$\propto(\partial_x I)^2$] and flattening ($\propto\partial_x^2 I$). Combined together, they facilitate the formation of a front, which separates the domains of the different homogeneous solutions (Fig. 2).[19,20] Thus, the "inner"- and "outer" solutions can be discussed separately. First, we discuss the local turbulence excitation process, i.e., the outer solution. By "turning off" the inhomogeneous term, Eq. (6) can be written in the variational form as

$$\frac{\partial}{\partial t}I = -\frac{\delta F(I)}{\delta I}, \tag{7}$$

where the potential F is

$$F(I) = -\frac{1}{2}\gamma_0(\langle A\rangle - A_C)I^2 - \frac{2}{5}\sqrt{\frac{\gamma_0^2 D_0\langle A\rangle^2}{\chi_{neo}+|\chi_m|}}I^{5/2} + \frac{1}{3}\gamma_{nl}I^3. \tag{8}$$

For the subcritical case ($\langle A\rangle < A_C$), it is straightforward to show that Eq. (7) has two stable steady solutions. Setting $\delta F/\delta I = 0$, these follow as

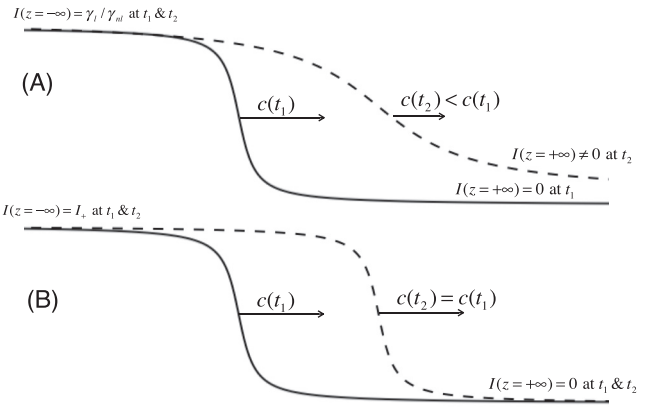

FIG. 2. (a) Turbulence front in the Fisher equation based model and the front is modified by local growth; (b) turbulence front in the bistability model. $c(t)$ is the front speed at t and $t_2 > t_1$.

$$I = 0 \quad \text{and} \quad I = I_+, \tag{9}$$

with the stable excited solution

$$I_+ = \frac{9\gamma_0^2 D_0\langle A\rangle^2}{25\gamma_{nl}^2\chi_{total}}\left(1+\sqrt{1+\frac{25\gamma_{nl}\chi_{total}}{6\gamma_0 D_0\langle A\rangle^2}(\langle A\rangle - A_C)}\right)^2 \tag{10}$$

and one unstable solution

$$I_- = \frac{9\gamma_0^2 D_0\langle A\rangle^2}{25\gamma_{nl}^2\chi_{total}}\left(1-\sqrt{1+\frac{25\gamma_{nl}\chi_{total}}{6\gamma_0 D_0\langle A\rangle^2}(\langle A\rangle - A_C)}\right)^2, \tag{11}$$

where $\chi_{total} \equiv \chi_{neo} + |\chi_m|$. In other words, by including the temperature corrugation effect, the unistable system [Eq. (1)] is replaced by one which is bistable. Typically, one has $F(I_+) < F(0)$, so the laminar state $I = 0$ is *metastable*, while the excited state $I = I_+$ is *absolutely stable* (Fig. 3). Equation (10) implies that the excited turbulence intensity $\propto\langle A\rangle^2$ has a stronger scaling than the Fisher model [$\propto(\langle A\rangle - A_C)$].

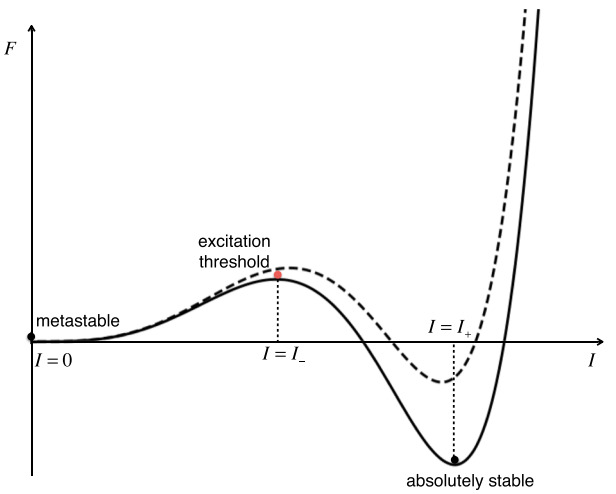

FIG. 3. Configuration of the potential energy $F(I)$. Dashed curve: impact of mean $E\times B$ shear on $F(I)$.

To initiate local excitation, I must exceed a threshold $I_C = I_-$, which is set by the height of the potential barrier of F (Fig. 3).

We thus have arrived a physics picture where the system given by Eq. (7) can be viewed as a "sea" of laminar ($I = 0$) and excited ($I = I_+$) domains. To understand how these domains are connected, one needs to incorporate the spatial coupling term in Eq. (6). For a front (i.e., the inner solution), one has $I(x, t) = I(z)$ with $z = x - c^* t$ (c^*:speed of the front propagation). Equation (6) becomes

$$-c^* \frac{d}{dz} I = -\frac{\delta F}{\delta I} + D_1 I \frac{d^2}{dz^2} I + D_1 \left(\frac{d}{dz} I\right)^2. \tag{12}$$

c^* is also the eigenvalue of Eq. (12). Multiplying $\frac{d}{dz} I$ on both sides of Eq. (12) and integrating from $z = -\infty$ to $z = +\infty$ yield

$$c^* = \frac{F(+\infty) - F(-\infty)}{\int_{-\infty}^{+\infty} I'^2 dz} + \frac{-\frac{D_1}{2}\int_{-\infty}^{+\infty} I'^3 dz}{\int_{-\infty}^{+\infty} I'^2 dz}, \tag{13}$$

where $I' \equiv dI/dz$. The propagation of the front is driven by two effects: (1) the free energy difference of the two homogeneous states and (2) the spatial steepening of the turbulence intensity due to nonlinear diffusion. For the type of front sketched in Fig. 1, one has $F(+\infty) - F(-\infty) = F(0) - F(I_+) > 0$ (Fig. 3) and $I' < 0$, so that both effects make a positive contribution to c^*. Since Eq. (12) is invariant under the transformations $I' \to -I'$ and $c^* \to -c^*$, the front with $F(+\infty) = F(I_+)$ and $F(-\infty) = F(0)$ has a propagating velocity $-c^*$. A simple observation of Eq. (13) is that c^* has a basic structure $c^* = aL + \frac{b}{L}$ with a and b being constant (determined by the turbulence intensity) and L the characteristic size of the front layer. Then, one can expect that there exists a lower limit on the velocity of the front, $c^* \geq 2\sqrt{ab} \equiv c_{min}$.[21] An exact solution of Eq. (12) is not crucial here. We instead pursue the basic scaling of c_{min} for the near marginal scenario. After the re-scalings $I \to \frac{\gamma_0^2 D_0}{\gamma_{nl}^2(\chi_{neo}+|\chi_m|)} \langle A\rangle^2 I$, $x \to \sqrt{\frac{D_0}{\gamma_{nl}}} x, t \to \frac{\gamma_{nl}(\chi_{neo}+|\chi_m|)}{\gamma_0^2 D_0 \langle A\rangle^2} t$, Eq. (12) is dimensionless. The scaling of the minimal front speed follows as

$$c^* \geq c_{min} \propto \frac{\gamma_0^2 \langle A\rangle^2 D_0}{\gamma_{nl}(\chi_{neo} + |\chi_m|)} \sqrt{\frac{D_0}{\gamma_{nl}}} \sim V_{*e} \frac{\omega_{*e}}{\Delta\omega} k_y l_{mix}, \tag{14}$$

where the basic scalings of drift wave turbulence $\gamma_0 \langle A\rangle \propto \omega_{*e} = k_y V_{*e}$($V_{*e}$: electron diamagnetic drift velocity and k_y: poloidal wave number), $D_0 \simeq \chi_{GB}$ (Bohm-like thermal conductivity), $\gamma_{nl} \simeq \Delta\omega$ (frequency spectrum width), and approximations $|\chi_m| \gg \chi_{neo}$, $|\chi_m| \sim \chi_{GB}$ were used. $l_{mix} \equiv \sqrt{D_0/\gamma_{nl}}$ is the mixing length (or characteristic wavelength) of the drift wave turbulence. Evidently, the outer solutions [$I(z = -\infty)$ and $I(z = +\infty)$] of the bistable front are stable. The stability of the inner solution is unclear and requires further analysis. In fact, an unstable inner solution would induce the splitting of the front and hence facilitate the spreading of the turbulence. The possibility for the existence of a unstable inner solution is an interesting topic to explore in the future.

The linear dissipation effect of the mean $E \times B$ shear can be incorporated directly into this bistable turbulence spreading model. This can up-shift the critical temperature gradient A_C, so that the extent of the subcritical region is enlarged.[22] Excitation of the turbulence fluctuations then becomes harder (Fig. 3), and the amplitude of I_+ is decreased. For a strong enough mean $E \times B$ shear (or transport barrier), the relative stability of the laminar- and excited states can be reversed, i.e., the excited state can become metastable and the laminar state becomes absolutely stable, so that the system tends to evolve to a laminar state (as in a transport barrier). So, the bistable model for turbulence excitation and spreading also provides a stimulating framework for understanding transition processes between L- and H modes. Through the residual term of Reynolds stress,[23] the energy of the turbulence can be coupled to the parallel flow; one can expect that the parallel flow shear would induce a nonlinear saturation effect to I's evolution and hence reduce the amplitude of the excited solution and the spreading speed of the front.

We are grateful to Ö.D. Gürcan for useful discussions. We also acknowledge fruitful interactions with participants in the 2015 and 2017 Festival de Théorie, Aix-en- Provence. This work was supported by the Department of Energy under Award No. DE-FG02-04ER54738.

[1]X. Garbet, L. Laurent, A. Samain, and J. Chinardet, Nucl. Fusion **34**, 963 (1994).
[2]T. S. Hahm, P. H. Diamond, Z. Lin, K. Itoh, and S. I. Itoh, Plasma Phys. Controlled Fusion **46**, A323 (2004).
[3]Ö. D. Gürcan, P. H. Diamond, T. S. Hahm, and Z. Lin, Phys. Plasmas **12**, 032303 (2005).
[4]W. X. Wang, T. S. Hahm, W. W. Lee, G. Rewoldt, J. Manickam, and W. M. Tang, Phys. Plasmas **14**, 072306 (2007).
[5]S. Yi, J. Kwon, P. Diamond, and T. Hahm, Phys. Plasmas **21**, 092509 (2014).
[6]Y. Pomeau, Phys. D **23**, 3–11 (1986).
[7]T. Estrada, C. Hidalgo, and T. Happel, Nucl. Fusion **51**, 032001 (2011).
[8]X. Garbet, Y. Sarazin, F. Imbeaux, P. Ghendrih, C. Bourdelle, Ö. D. Gürcan, and P. H. Diamond, Phys. Plasmas **14**, 122305 (2007).
[9]R. E. Waltz, M. E. Austin, K. H. Burrell, and J. Candy, Phys. Plasmas **13**, 052301 (2006).
[10]J. Lang, S. E. Parker, and Y. Chen, Phys. Plasmas **15**, 055907 (2008).
[11]D. G. Dritschel and M. E. McIntyre, J. Atmos. Sci. **65**, 855–874 (2008).
[12]S. Inagaki, T. Tokuzawa, N. Tamura, S.-I. Itoh, T. Kobayashi, K. Ida, T. Shimozuma, S. Kubo, K. Tanaka, T. Ido, A. Shimizu, H. Tsuchiya, N. Kasuya, Y. Nagayama, K. Kawahata, S. Sudo, H. Yamada, A. Fujisawa, K. Itoh, and the LHD Experiment Group. Nucl. Fusion **53**, 113006 (2013).
[13]B. B. Kadomtsev and O. P. Pogutse, *Reviews of Plasma Physics* (Springer, US, 1970).
[14]A. Ashourvan and P. H. Diamond, Phys. Rev. E **94**, 051202 (2016).
[15]Y. Kosuga, P. H. Diamond, and Ö. D. Gürcan, Phys. Rev. Lett. **110**, 105002 (2013).
[16]L. Bardoczi, T. L. Rhodes, N. A. Banon, C. Sung, T. A. Carter, R. J. La Haye, G. R. McKee, C. C. Petty, C. Chrystal, and F. Jenko, Phys. Plasmas **24**, 056106 (2017).
[17]F. Paparella and J. Hardenberg, Acta Applicandae Math. **132**, 457–467 (2014).
[18]Y. B. Zel'dovich, Sov. Phys. JETP **4**, 460–462 (1957).
[19]M. Kardar, G. Parisi, and Y. C. Zhang, Phys. Rev. Lett. **56**, 889 (1986).
[20]P. H. Diamond and T. S. Hahm, Phys. Plasmas **2**, 3640–3649 (1995).
[21]F. Sanchezgarduno and P. K. Maini, J. Differ. Equations **117**, 281–319 (1995).
[22]E. G. Highcock, M. Barnes, A. A. Schekochihin, F. I. Parra, C. M. Roach, and S. C. Cowley, Phys. Rev. Lett. **105**, 215003 (2010).
[23]Ö. D. Gürcan, P. H. Diamond, P. Hennequin, C. J. McDevitt, X. Garbet, and C. Bourdelle, Phys. Plasmas **17**(11), 112309 (2010).